International Symposium
On Turbulence and Shear Flow
Phenomena (TSFP-9)
June 30 - July 3, 2015 *Melbourne, Australia*

UNIFIED RANS-LES METHOD BASED ON SECOND-ORDER CLOSURE

Michael Stoellinger,
Department of Mechanical Engineering,
University of Wyoming
1000 E. Univ. Ave., Laramie WY 82071, USA
mstoell@uwyo.edu

Rajib Roy
Department of Mechanical Engineering,
University of Wyoming
1000 E. Univ. Ave., Laramie WY 82071, USA
rroy@uwyo.edu

Stefan Heinz
Department of Mathematics,
University of Wyoming
1000 E. Univ. Ave., Laramie WY 82071, USA
heinz@uwyo.edu

ABSTRACT

The feasibility of using a second order closure model based on the elliptic blending Reynolds stress model (RSMeb) in a unified RANS-LES approach is investigated in this paper. The advantage of the RSMeb is that it does not use any geometrical wall distance or wall normal vector information which makes it well suited for application in flows with complex wall geometries. The original RANS model is slightly modified and is then extended to a unified RANS-LES model based on the partially integrated transport method (PITM). The unified RANS-LES model is applied in a flow over a periodic hill and in a flow over a NACA 4412 airfoil with trailing edge separation. Both flows display separation and non-equilibrium effects. The unified RSMeb model operates as RANS model near the surface in the attached region and smoothly transitions towards LES in separated region and in the wake. The model provides results that are in good agreement with the available experimental data and in general the result are improved as compared to pure RANS results.

INTRODUCTION

The development of so called hybrid RANS-LES models that attempt at combining the advantages of the RANS and LES modeling approaches has been a research focus for more than decade. Different models have emerged such as the Detached Eddy Simulation (DES) method of Spalart (2009), the Scale Adaptive Simulation (SAS) method of Menter & Egorov (2005), the Partially Averaged Navier-Stokes (PANS) method of Girimaji (2006), the Partially Integrated Transport Model PITM of Fadai-Ghotbi *et al.* (2010), Chaouat & Schiestel (2012) or the unified RANS-LES model of Heinz (2007) and Gopalan *et al.* (2013) to name a few. Most of these methods are based on one-equation models (e.g. DES) or two-equation models that invoke the eddy-viscosity assumption for the modeled turbulence stress. When applied in wall bounded flows, these models are usually integrated to the wall but still need a damping function to yield the correct shear stress in the log-layer. A notable exception here is the PANS approach based on the $k-\varepsilon-\zeta-f$ model of Basara *et al.* (2011). In flows with stagnation points (e.g. aerodynamics applications) the eddy viscosity model leads to an excessive production of turbulence kinetic energy and hence limiters have to be introduced (Durbin (2009)). Turbulence models based on second-moment closure directly solve modeled transport equations for the Reynolds stress and thus do not need to invoke the eddy-viscosity assumption. However, the main modeling issue related to the pressure redistribution term is usually addressed for nearly homogeneous flows and hence the redistribution models need to be modified to be applicable to wall bounded flows. The effect of kinematic blocking on the redistribution term and its elliptic nature was successfully modeled by Durbin (1993) using the so called elliptic relaxation model. The elliptic relaxation model is based on the solution of six elliptic equations to adjust any homogeneous redistribution model to yield the correct near wall behavior. More recently, a simpler albeit slightly less accurate model that solves only one additional elliptic equation was proposed by Manceau & Hanajalić (2002), Thielen *et al.* (2005) and R. Manceau (2014). The model is based on a blending between any homogeneous redistribution model like the SSG model (Speziale *et al.* (1991)) and a near wall redistribution model that has the desired asymptotic behavior. The blending variable is based on the solution of an elliptic equation. No geometric wall distance variable is needed which makes the elliptic blending model particular suitable for flows with complex geometries. It should be noted that an elliptic blending RSM (RSMeb) model was adopted using the PITM approach of Fadai-Ghotbi *et al.* (2010) to perform unified RANS-LES simulations of a channel flow at low Reynolds number. The aim of this paper is to further investigate the potential of the RSMeb model in unified RANS-LES simulations of flows with separation.

UNIFIED RANS-LES MODEL

The unified RANS-LES model for an incompressible fluid is based on the spatially filtered (filter size Δ) Navier-Stokes equations

$$\frac{\partial \overline{u}_i}{\partial x_j} = 0 \tag{1}$$

and,

$$\frac{\partial \overline{u}_i}{\partial t} + \overline{u}_j \frac{\partial \overline{u}_i}{\partial x_j} = -\frac{1}{\rho}\frac{\partial \overline{p}}{\partial x_i} + \nu \frac{\partial^2 \overline{u_i}}{\partial x_j \partial x_j} - \frac{\partial \tau_{ij}}{\partial x_j}, \tag{2}$$

where $\overline{u}_i$ is the filtered velocity, ρ is the constant density, $\overline{p}$ is the filtered pressure and $\tau_{ij} = \overline{u_i u_j} - \overline{u}_i \overline{u}_j$ denotes the modeled sub-grid scale (SGS) stress. The filter scale Δ is related to the grid cells through an expression developed by Scotti *et al.* (1993)

$$\Delta = V_c^{\frac{1}{3}} \cosh\left(\sqrt{4/27\left[(\ln a_1)^2 - \ln a_1 \ln a_2 + (\ln a_2)^2\right]}\right), \tag{3}$$

where V_c is the volume of the cell and, a_1 and a_2 are the aspect ratios of the cell. Here we extend the concept of aspect ratios to arbitrary cells by defining the aspect ratios to be $a_1 = A_{min}/A_{max}$ and $a_2 = A_{min}/A$ where A_{min}, A_{max}, and A are the minimum cell face area, the maximum cell face area and the second smallest cell face area, respectively. It is straightforward to show that for anisotropic Cartesian grids the definition of Scotti *et al.* (1993) is recovered.

The transport equation for the SGS stress is modeled based on the RSMeb model recently presented by Roy & Stoellinger (2015). The SGS stress model is formulated in terms of the homogeneous dissipation rate ε^h as suggested by Jakirlić & Hanjalić (2002):

$$\begin{aligned}\frac{\partial \tau_{ij}}{\partial t} + \overline{u}_j \frac{\partial \tau_{ij}}{\partial x_j} &= P_{ij} + \Phi^*_{ij} - \varepsilon^h_{ij} \\ &+ \frac{\partial}{\partial x_k}\left[\left(0.5\nu\delta_{kl} + C_k \frac{k}{\varepsilon^h}\tau_{kl}\right)\frac{\partial \tau_{ij}}{\partial x_l}\right],\end{aligned} \tag{4}$$

where P_{ij} is the production, Φ^*_{ij} is the pressure redistribution term, ε^h_{ij} is the homogeneous dissipation rate tensor and the last term represents molecular diffusion and turbulent transport according to the Daly & Harlow (1970) model with $C_k = 0.21$. The factor of one half for the molecular diffusion term results from the use of the homogeneous dissipation rate

$$\varepsilon^h = \varepsilon - 0.5\nu \frac{\partial^2 k}{\partial x_l x_l}, \tag{5}$$

where the SGS kinetic energy is $k = \tau_{ll}/2$. The production term is given by

$$P_{ij} = -\tau_{ik}\frac{\partial \overline{u}_j}{\partial x_k} - \tau_{jk}\frac{\partial \overline{u}_i}{\partial x_k}. \tag{6}$$

In the elliptic blending approach (Manceau & Hanajalić (2002)) the redistribution term is given by a "linear blending" of a near wall model Φ^w_{ij} and a homogeneous model Φ^h_{ij} that is appropriate away from the wall

$$\Phi^*_{ij} = (1 - f_\alpha)\Phi^w_{ij} + f_\alpha \Phi^h_{ij}, \tag{7}$$

where $f_\alpha = \alpha^3$ is the blending function which is based on the variable α that defines the "closeness" to a solid wall and that satisfies an elliptic equation (R. Manceau (2014)):

$$\alpha - L_d^2 \nabla^2 \alpha = 1. \tag{8}$$

The boundary conditions are such that at solid walls $\alpha = 0$ and in the freestream $\alpha = 1$. The length scale L_d is chosen as the maximum value between a large scale turbulence length scale and the Kolmogorov length scale. The Kolmogorov scale is used as a lower bound for the length scale to prevent the elliptic equation for α to become singular at the wall. In the unified RANS-LES implementation, for fine grids that behave almost like a well resolved LES, there is a significant amount of resolved dissipation and hence the Kolmogorov length scale calculated based solely on the modeled dissipation rate ε^h would be greatly over predicted. In fact, in such a highly resolved case most of the wall blocking effect is directly accounted for through the pressure boundary condition. Only the sub-grid scales require modeling of the wall blocking and the corresponding length scale Δ is quite well approximated by the local instantaneous value of $k^{3/2}/\varepsilon^h$. Thus, the equation for the length scale L_d for regions that are sufficiently well resolved is modified by using a threshold value for turbulence kinetic energy ratio $r_{k,e}$ (defined below):

$$L_d = \begin{cases} max\left(C_L \frac{k^{3/2}}{\varepsilon^h}, C_\eta \frac{\nu^{3/4}}{(\varepsilon^h)^{1/4}}\right) & \text{if } r_{k,e} > 0.5, \\ C_L \frac{k^{3/2}}{\varepsilon^h} & \text{otherwise,} \end{cases} \tag{9}$$

with constants $C_L = 0.13$ and $C_\eta = 10$.

The dissipation rate tensor is given by a blending between the near wall anisotropic form and the common isotropic form far away from the wall

$$\varepsilon^h_{ij} = (1 - f_\alpha)\frac{\tau_{ij}}{k}\varepsilon^h + f_\alpha \frac{2}{3}\varepsilon^h \delta_{ij}. \tag{10}$$

The homogeneous part of the redistribution term is modeled according to the SSG model (Speziale *et al.* (1991))

$$\begin{aligned}\Phi^h_{ij} = &-\left(C_{g1} + C^*_{g1}\frac{P}{\varepsilon^h}\right)\varepsilon^h a_{ij} + C_{g2}\left(a_{ik}a_{kj} - \frac{1}{3}a_{kl}a_{kl}\delta_{ij}\right) \\ &+ \left(C_{g3} - C^*_{g3}\sqrt{a_{kl}a_{kl}}\right)kS_{ij} + C_{g5}k\left(a_{ik}\Omega_{jk} + a_{jk}\Omega_{ik}\right) \\ &+ C_{g4}k\left(a_{ik}S_{jk} + a_{jk}S_{ik} - \frac{2}{3}a_{lm}S_{lm}\delta_{ij}\right),\end{aligned} \tag{11}$$

where $P = P_{kk}/2$ is the production of turbulent kinetic energy, $a_{ij} = \tau_{ij}/k - 2/3\delta_{ij}$ is the anisotropy tensor, $S_{ij} = \frac{1}{2}\left(\frac{\partial \overline{u}_i}{\partial x_j} + \frac{\partial \overline{u}_j}{\partial x_i}\right)$ is the rate-of-strain tensor, and $\Omega_{ij} = \frac{1}{2}\left(\frac{\partial \overline{u}_i}{\partial x_j} - \frac{\partial \overline{u}_j}{\partial x_i}\right)$ is the rate-of-rotation tensor. The model coefficients are $C_{g1} = 1.7$, $C^*_{g1} = 0.9$, $C_{g2} = 1.05$, $C_{g3} = 0.8$, $C^*_{g3} = 0.65$, $C_{g4} = 0.625$, $C_{g5} = 0.2$. The near wall form of the redistribution model was derived in Manceau & Hanajalić (2002) such that the correct asymptotic near-wall behavior is obtained

$$\Phi^w_{ij} = -5\frac{\varepsilon^h}{k}\left(\tau_{ik}n_j n_k + \tau_{jk}n_i n_k - \frac{1}{2}\tau_{kl}n_k n_l\left(n_i n_j + \delta_{ij}\right)\right), \tag{12}$$

where the wall normal vector $\vec{n}$ is obtained from the elliptic

variable α through

$$\vec{n} = \frac{\nabla\alpha}{\|\nabla\alpha\| + 10^{-10}}, \tag{13}$$

such that the normal vector becomes the zero vector far away from the wall. The closure of the dissipation rate equation follows the proposal of Jakirlić & Hanjalić (2002) but modified with a simplified term for the viscous near wall production:

$$\begin{aligned}\frac{\partial\varepsilon^h}{\partial t} + \overline{u}_j\frac{\partial\varepsilon^h}{\partial x_j} &= C_{\varepsilon 1}P\frac{\varepsilon^h}{k} - C_{\varepsilon 2,sfs}f_\varepsilon\frac{\tilde{\varepsilon}^h\varepsilon^h}{k} + E_\varepsilon \\ &+ \frac{\partial}{\partial x_k}\left[\left(0.5\nu\delta_{kl} + C_\varepsilon\frac{k}{\varepsilon^h}\tau_{kl}\right)\frac{\partial\varepsilon^h}{\partial x_l}\right],\end{aligned} \tag{14}$$

with

$$E_\varepsilon = 2C_{\varepsilon 3}\nu\frac{k^2}{\varepsilon^h}(1-\alpha)\left(\frac{\partial^2\overline{u}_i}{\partial x_k\partial x_k}\right)^2. \tag{15}$$

The term $(1-\alpha)$ in (15) ensures that the viscous production term is only active near the wall and

$$\tilde{\varepsilon}^h = \varepsilon^h - \nu\left(n_i\frac{\partial\sqrt{k}}{\partial x_i}\right)^2, \tag{16}$$

ensures that $\tilde{\varepsilon}^h = \varepsilon^h$ far from the wall. The function f_ε is modified from a Re_t dependent formulation of Jakirlić & Hanjalić (2002) to be a function of the elliptic near wall variable α and is given by

$$f_\varepsilon = 1 - \frac{C_{\varepsilon 2} - C_{\varepsilon 1}}{C_{\varepsilon 2}}\exp\left[-(7\alpha)^5\right]. \tag{17}$$

The model coefficients for the homogeneous dissipation rate equation are

$$C_{\varepsilon 1} = 1.44,\ C_{\varepsilon 2} = 1.82,\ C_{\varepsilon 3} = 0.005,\ C_\varepsilon = 0.18. \tag{18}$$

The unified RSMeb model is based on the PITM approach to allow for a smooth transition from a statistical (or RANS) model to a LES model through modifying the destruction term in the dissipation rate equation. The modification accounts for the fact that in the case some of the turbulence is resolved the length of the spectral transfer range is reduced and hence the model coefficient of the destruction term should be reduced accordingly (Chaouat & Schiestel (2009)). The modified coefficient is given by

$$C_{\varepsilon 2,sfs} = C_{\varepsilon 1} + r_{k,e}\left(C_{\varepsilon 2} - C_{\varepsilon 1}\right), \tag{19}$$

where $r_{k,e}$ is the resolved to total turbulence kinetic energy ratio. Chaouat & Schiestel (2009) related this ratio to a turbulence macro scale L_e and the filter scale Δ using a modeled turbulence spectrum that is valid in the low wave number range and recovers the Kolmogorov $-5/3$ behavior for large wave numbers κ. The modeled expression is given by

$$r_{k,e} = \frac{1}{\left[1 + \beta_\eta\eta_c^3\right]^{2/9}}, \tag{20}$$

where $\beta_\eta = 0.0495$ is a model coefficient and η_c is the non-dimensional spectral cut-off frequency

$$\eta_c = \kappa_c L_e = \frac{\pi}{\Delta}L_e. \tag{21}$$

The turbulence length scale L_e in equation (21) is given by

$$L_e = \frac{k_{tot}^{3/2}}{\varepsilon_{tot}}, \tag{22}$$

where the total turbulence kinetic energy is given by $k_{tot} = \langle k\rangle_{TA} + k_{res}$ where $\langle k\rangle_{TA}$ is a running time average of the modeled SGS kinetic energy $k = \tau_{ll}/2$ and the resolved part of the turbulence kinetic energy is $k_{res} = (\langle\overline{u}_l\overline{u}_l\rangle_{TA} - \langle\overline{u}_l\rangle_{TA}\langle\overline{u}_l\rangle_{TA})/2$. To account for the low Reynolds number turbulence near a wall the dissipation rate in the length scale L_e is also calculated as a sum of the modeled and resolved dissipation rates $\varepsilon_{tot} = \langle\varepsilon\rangle_{TA} + \varepsilon_{res}$, where ε is calculated from equation (5) and the resolved dissipation rate is obtained from

$$\varepsilon_{res} = \nu\left(\left\langle\frac{\partial\overline{u}_i}{\partial x_j}\frac{\partial\overline{u}_i}{\partial x_j}\right\rangle_{TA} - \frac{\partial\langle\overline{u}_i\rangle_{TA}}{\partial x_i}\frac{\partial\langle\overline{u}_i\rangle_{TA}}{\partial x_i}\right). \tag{23}$$

The running time average of any variable $Q(t)$ at time t is based on an exponentially weighted average defined by

$$\begin{aligned}\langle Q\rangle_{TA}(t) &= c_{av}\langle Q\rangle_{TA}(t-\Delta t) + (1-c_{av})Q(t), \\ c_{av} &= \frac{1}{1+\frac{\Delta t}{T_{av}-\Delta t}},\end{aligned} \tag{24}$$

where Δt is the simulation time-step and T_{av} is a prescribed averaging time scale.

The boundary conditions at the walls are given by:

$$\overline{u}_i = 0,\ \tau_{ij} = 0,\ \varepsilon^h = \nu\frac{k}{y_1^2},\ \alpha = 0, \tag{25}$$

where y_1 is the wall normal distance of the first cell center. It should be noted that the above model is neither dependent on a geometrically defined wall distance and wall normal direction nor dependent on turbulence Reynolds number.

UNIFIED MODEL RESULTS

The performance of the unified RANS-LES method based on the RSMeb sub-grid scale model is investigated using simulations for two cases: the periodic hill flow and the flow over a NACA 4412 airfoil with trailing edge separation.

Periodic hill flow

The periodic hill flow test case is adopted from Mellen *et al.* (2000). It is a channel with a periodic hill and valley at the bottom. For a given hill peak height h, the maximum channel height is $3.035h$. The hill spans $4h$ and the valley spans $5h$, (i.e. at every $9h$ the geometry repeats itself). Such a configuration allows for flow separation and reattachment even in low Reynolds number flows. The simulations have been performed for a Reynolds number $Re_b = 37{,}000$ based on bulk velocity U_b and hill height h. The computational domain extends $9h \times 3.035h \times 4.5h$ in streamwise, wallnormal and spanwise direction, respectively. The grid is made of $200\times100\times100$ structured cells such that $y^+ < 1$ on both channel walls. Periodic boundary conditions are applied in the streamwise and spanwise direction. The top and bottom

walls are considered as no-slip walls. A uniform pressure gradient is added to the momentum conservation equation to maintain a constant mass flow rate. Fig. 1 illustrates the geometry with typical flow streamlines displaying the flow separation and reattachment regions.

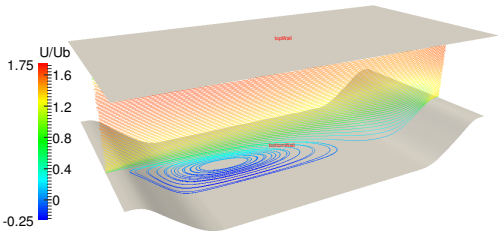

Figure 1. Periodic hill geometry and streamwise mean velocity normalized by bulk channel velocity (U_b).

The unified RSMeb model is implemented in the open source finite volume CFD software OpenFOAM. The incompressible solver is based on the PISO pressure-velocity coupling and second order accurate schemes based on linear interpolation (corresponding to central differences) for spatial discretization are used unless stated otherwise. The time discretization of all equations is based on a second order accurate backward scheme and to keep the time discretization and splitting errors small the Courant number is limited to $Co < 0.1$. The convective term in the momentum conservation equation is discretized by 2^{nd} order accurate Gamma scheme with 20% upwinding limit and the convection terms in the SGS stress τ_{ij} and dissipation rate ε^h equations are discretized with a 1^{st} order upwind scheme. The flow was initialized with a 2D RANS solution onto which Gaussian perturbations with an intensity of 20% have been added to accelerate the transition to a 3-D flow field. The averaging time scale for the running time average T_{av} has been set to three flow-through times $T_{av} = 3 \cdot (9h/U_b)$. After an initial transient period, time averages have been calculated over six flow through times and are further averaged over the statistically homogeneous spanwise direction.

In Figure 2 the streamwise mean velocity obtained with the RANS-RSMeb model and the unified RSMeb model is compared to experimental results and the LES results of Breuer *et al.* (2009) at locations $x/h = 2$ (end of hill) and $x/h = 4$ (close to reattachment). The unified model results are in good agreement with the experimental data and indeed display a significant improvement over the pure RANS-RSMeb model results. Comparisons of the streamwise normal stress ($\overline{u'u'}$) and the shear stress ($\overline{u'v'}$) are illustrated in Figure 3. The stress in the unified model is obtained as the sum of the modeled and resolved stress contributions (both of which are shown as well). For both components of the stress tensor the modeled stress dominates only very close to the top wall (near wall RANS region) similar to the findings of Chaouat & Schiestel (2013) in their PITM study of the periodic hill flow. This means that the resolution at the top wall with the adopted grid would be too coarse for a wall-resolved LES and hence a wall resolved LES would require a much finer grid. Away from the walls, the resolved stress becomes dominant indicating sufficient resolution for LES. The total stresses predicted by the unified model are in good agreement with the experimental and wall-resolved LES data of Breuer *et al.* (2009) and provides a significant improvement over the RANS-RSMeb model results.

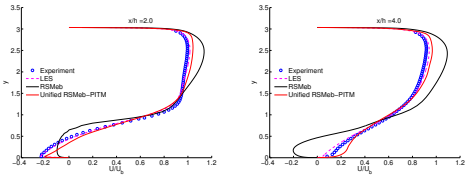

Figure 2. Streamwise mean velocity comparison with experimental and LES results at location $x/h = 2$ (left) and $x/h = 4$ (right) for the periodic hill flow.

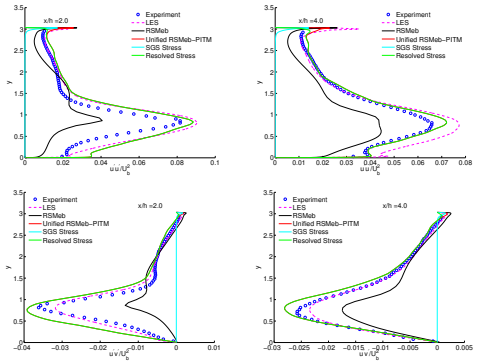

Figure 3. Streamwise normal stress (top) and shear stress (bottom) comparison with experimental and LES results at location $x/h = 2$ (left) and $x/h = 4$ (right) for the periodic hill flow.

2D NACA 4412 trailing edge separation

The experimental study of Wadcock (1987) displays trailing edge separation of the 2D NACA 4412 airfoil at maximum lift configuration (angle of attack 12^o). The experiment was performed with an airfoil chord length of $c = 0.9m$, chord length based Reynolds number 1.64×10^6 with free-stream velocity 29.1 m/s (Mach number 0.085) and these parameters were retained in the performed simulation. In the experiment, a free-stream turbulence intensity of 0.25% to 0.85% was observed and the higher value is used for the inlet condition in the simulation. Although the airfoil boundary layer was tripped in the experiment, the simulation has been performed without a trip as the boundary layer promptly transitions to fully turbulent right after the stagnation point. To account for the blockage effect of the wind tunnel, the computational domain replicates the wind tunnel test section height (2.1336 m or 7 ft.). The airfoil is placed $6.35cm(2.5inch)$ below from the centerline to mimic the experimental setup. The experimental test section was only 4.572m (15 ft.) long but the adopted computational domain extends 7.78 chords (7m) upstream of the airfoil leading edge and 8.89 chords (8m) downstream. The upstream extension ensures a close to zero pressure gradient which is essential for the adopted fixed velocity-inlet boundary condition. The downstream extension allows for

airfoil-wake pressure recovery and resembles an ideal ambient pressure-outlet boundary condition. Wadcock (1987) reported a thin boundary layer at the tunnel walls compared to the wind tunnel height and in the current simulations the "top" and "bottom" walls are considered as slip-wall. A periodic boundary condition is adopted in the spanwise direction. A multi-block structured grid of approx. $100,000$ quadrilaterals in 2D is extruded in the spanwise direction to a length of $c/3$ using 120 cells (total of $12M$ hexahedral cells). Fig. 4 illustrates the boundary layer resolved structured grid around the airfoil. A maximum value $y^+ = 2.63$ is observed at the leading edge and the average y^+ is 0.94.

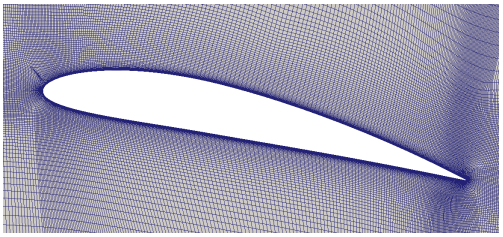

Figure 4. Boundary-layer resolved structured mesh around the NACA 4412 airfoil.

The convective term in the momentum conservation equation is discretized by the 2^{nd} order accurate Gamma scheme with a 20% upwinding limit and the convective terms in the SGS stress and dissipation rate equations use Gamma schemes with 50% upwinding limit. The flow was initialized with a 2D RANS result onto which Gaussian perturbations with an intensity of 20% have been added to accelerate the transition to a 3-D flow field. The averaging time scale for the running time average T_{av} has been set as two flow over chord times $T_{av} = 2c/U_\infty$ which leads to $c_{av} = 0.99998333$. After an initial transient period, time averages have been obtained over six chord times and are further averaged over the homogeneous spanwise direction for post-processing. Table 1 shows that the unified RSMeb model accurately predicts the coefficient of lift and the location of separation. The coefficient of drag is still under predicted in the unified simulation but the error is reduced to almost half of the error of the pure RANS-RSMeb model result. Fig. 5 depicts a more detailed comparison

Int. values	C_D (*err%*)	C_L (*err%*)	$x/c_{sep.}$ (*dev.*(x/c))
Exp.	0.0423	1.450	0.815
RSMeb	0.0257 (39.2)	1.544 (22.7)	0.884 (0.07)
Unified	0.0327 (22.7)	1.468 (1.27)	0.795 (0.02)

Table 1. Comparison of RANS-RSMeb and unified RSMeb-PITM model results with experimental data of Coefficient of Drag, Coefficient of Lift and location of separation for the 2D NACA 4412 trailing edge separation case.

between experimental results, unified RSMeb results and pure RANS results at $x/c = 0.815$ (onset of separation) and $x/c = 0.952$ (within the separation zone) locations. The unified model accurately predicts the streamwise velocity. The total streamwise stress component predicted by the unified model is calculated as the sum of the modeled (SGS) and resolved contributions. In the unified model simulation, most of the attached flow over the airfoil is modeled as RANS as can be seen by the very small resolved stress contributions in fig. 5. Both, the pure RANS RSMeb results and the unified RSMeb results for the total stress are smaller then the experimental values. Fig. 6 shows the streamwise mean velocity and stresses in the wake of the airfoil at $x/c = 1.282$. Contrary to the boundary layer, in the airfoil wake most of the turbulent motion is resolved as can be seen by the resolved stress being significantly larger than the modeled part. The streamwise velocity in the wake is predicted significantly better by the unified model than by the RANS RSMeb model and the streamwise normal stress component is predicted reasonably well with both models. Fig. 7 il-

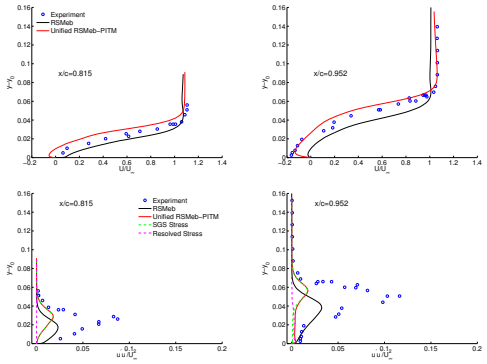

Figure 5. Streamwise mean velocity (upper) and normal stress (lower) plot of the Unified PITM-RSMeb and the RANS-RSMeb model compared to experimental data for the 2D NACA 4412 airfoil case at x/c = 0.815 and 0.952 respectively.

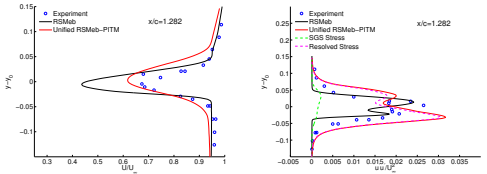

Figure 6. Streamwise velocity and normal stress plot of the Unified PITM-RSMeb and the RANS-RSMeb model compared to experimental data for the 2D NACA 4412 airfoil case at x/c = 1.282.

lustrates the trailing edge vortices by means of a $Q = 10s^{-2}$ iso-contour plot that is colored by the $C_{\varepsilon 2,sfs}$ values, which signifies the transition from a predominant RANS behavior to a predominant LES behavior. At the airfoil surface, most the flow is attached where the unified model operates mostly in RANS mode and the $C_{\varepsilon 2,sfs}$ value is close to the pure RANS value of 1.82. On the other hand, at the airfoil trailing edge the flow separates and ultimately produces a highly turbulent flow in the wake. Following the flow turbulence characteristics, the unified model gradually shifts towards LES which can be seen by smaller values $C_{\varepsilon 2,sfs} \approx 1.5$.

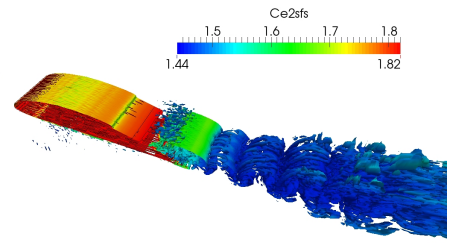

Figure 7. $Q = 10s^{-2}$ iso-contour plot colored by $C_{\varepsilon 2,sfs}$ values obtained form the unified RSMeb model for flow over 2D NACA 4412 airfoil with trailing edge separation.

SUMMARY

A unified RANS-LES model is developed based on the PITM approach with a second-moment closure using the elliptic blending approach. The elliptic blending formulation blends the pressure redistribution term linearly between a nearly isotropic model (far from wall) and a near wall anisotropic model. The model does not use any geometric wall distance or wall normal vector rather an elliptic variable α is solved for which is capable to follow complex wall geometries. The "closeness" to a solid wall is described by α and it is also used to define a wall-normal vector. The unified model smoothly transitions from RANS (in attached boundary layers) towards LES (in separated and well resolved regions) through a modified destruction coefficient in the dissipation rate equation according to the PITM approach. The unified RANS-LES model is applied in simulations of a periodic hill flow at $Re_b = 37,000$ and in a flow over a 2D NACA 4412 airfoil (aoa = 12^o) with trailing edge separation. For both flows, in the attached boundary layers very close to the wall the modeled stresses are dominant. Away from the wall, the resolved stresses become dominant and most of the turbulence is resolved. For both flows the mean streamwise velocity predicted by the unified model is in good agreement with the experimental results.

REFERENCES

Basara, B., Krajnovic, S., Girimaji, S. & Pavlovic, Z. 2011 Near-wall formulation of the partially averaged navier stokes turbulence model. *AIAA journal* **49** (12), 2627–2637.

Breuer, M., Peller, N., Rapp, C. & Manhart, M. 2009 Flow over periodic hills - numerical and experimental study over a wide range of reynolds numbers. *Computers and Fluids* **38**, 433–457.

Chaouat, B. & Schiestel, R. 2009 Progress in subgrid-scale transport modelling for continuous hybrid non-zonal rans/les simulations. *International Journal of Heat and Fluid Flow* **30** (4), 602–616.

Chaouat, B. & Schiestel, R. 2012 Analytical insights into the partially integrated transport modeling method for hybrid reynolds averaged navier-stokes equations-large eddy simulations of turbulent flows. *Physics of Fluids* **24** (8), 1–34.

Chaouat, B. & Schiestel, R. 2013 Hybrid RANS/LES simulations of the turbulent ow over periodic hills at high reynolds number using the PITM method. *Computers and Fluids* **84**, 279–300.

Daly, B. J. & Harlow, F. H. 1970 Transport equations in turbulence. *Physics of Fluids* **13**, 2634–2649.

Durbin, P. A. 1993 A reynolds stress model for near-wall turbulences. *Journal of Fluid Mechanics* **249**, 465–498.

Durbin, P. A. 2009 Limiters and wall treatments in applied turbulence modeling. *Fluid Dynamics Research* **41** (1), 012203.

Fadai-Ghotbi, A., Friess, C., Manceau, R. & Borée, J. 2010 A seamless hybrid rans-les model based on transport equations for the subgrid stresses and elliptic blending. *Physics of Fluids* **22**, 055104.

Girimaji, S.S. 2006 Partially-averaged navier-stokes model for turbulence: a reynolds-averaged navier-stokes to direct numerical simulation bridging method. *Journal of Applied Mechanics* **73**, 413.

Gopalan, H., Heinz, S. & Stöllinger, M. 2013 A Unified RANS-LES Model: Computational development, accuracey and cost. *Journal of Computational Physics* **249**, 249–274.

Heinz, S. 2007 Unified turbulence models for LES and RANS, FDF and PDF simulations. *Theoretical and Computational Fluid Dynamics* **21**, 99–118.

Jakirlić, S. & Hanjalić, K. 2002 A new approach to modelling near-wall turbulence energy and stress dissipation. *Journal of Fluid Mechanics* **459**, 139–166.

Manceau, R. & Hanajalić, K. 2002 Elliptic blending model: A new near-wall reynolds-stress turbulence closure. *Physics of Fluids* **14**, 744–753.

Mellen, C. P., Frohlic, J. & Rodi, W. 2000 Large Eddy Simulation of the flow over periodic hills. In *16th IMACS World Congress*.

Menter, FR & Egorov, Y. 2005 A scale-adaptive simulation model using two-equation models. In *43rd AIAA Aerospace Sciences Meeting and Exhibit*, pp. AIAA 2005–1095. Reno, Nevada.

R. Manceau 2014 Recent progress in the development of the elliptic blending reynolds-stress model. *International Journal of Heat and Fluid Flow* (0), in press.

Roy, R. & Stoellinger, M. 2015 Potential of the elliptic blending reynolds stress model for use in hybrid rans-les methods. *53rd AIAA Aerospace Sciences Meeting* **AIAA 2015-1982**, 1–17.

Scotti, A., Meneveau, C. & Lilly, D.K. 1993 Generalized Smagorinsky model for anisotropic grids. *Physics of Fluids A: Fluid Dynamics* **5**, 2306.

Spalart, P. R. 2009 Detached-eddy simulation. *Annual Review of Fluid Mechanics* **41**, 181–202.

Speziale, "C. G., Sarkar, S. & Gatski", T. B. 1991 Modelling the pressurestrain correlation of turbulence: an invariant dynamical systems approach. *Journal of Fluid Mechanics* **227**, 245–272.

Thielen, L., Hanjalic, K., Jonker, H. & Manceau, R. 2005 Predictions of flow and heat transfer in multiple impinging jets with an elliptic-blending second-moment closure. *International Journal of Heat and Mass Transfer* **48** (8), 1583–1598.

Wadcock, A. J. 1987 Investigation of Low-Speed Turbulent separated Flow around Airfoils. *Tech. Rep.* NASA-CR-177450. Ames Research Center,NASA.